Talanta 117 (2013) 412–418

Contents lists available at ScienceDirect

Talanta

journal homepage: www.elsevier.com/locate/talanta

# Naphthyridine-based lanthanide complexes worked as magnetic resonance imaging contrast for guanosine 5′-monophosphate *in vivo*

Jichuan Kong [a,b], Tao Liu [a], Yongming Bao [c], Kun Jin [a], Xiaolin Zhang [d], Qin Tang [c], Chunying Duan [a,*]

[a] State Key Laboratory of Fine Chemicals, Dalian University of Technology, 158 Zhongshan Road, Dalian 116012, PR China
[b] Institute of Physics and Chemistry, Henan Polytechnic University, 454000 Jiaozuo, PR China
[c] School of Life Science and Biotechnology, Dalian University of Technology, 116023 Dalian, PR China
[d] College of Environmental and Chemical Engineering, Dalian University, Dalian 116622, PR China

ARTICLE INFO

*Article history:*
Received 26 June 2013
Received in revised form
11 September 2013
Accepted 16 September 2013
Available online 25 September 2013

*Keywords:*
Chemosensor
Guanosine 5′-monophosphate
Magnetic resonance imaging
Naphthyridine
Gd

ABSTRACT

New lanthanide complex Gd**-ANAMD** containing 2-amino-7-methyl-1,8-naphthyridine was achieved for selective magnetic resonance imaging towards guanosine 5′-monophosphate over other ribonucleotide polyphosphates in aqueous media and *in vivo*. The formation of strong multi-hydrogen bonds between naphthyridine and guanosine made the phosphate in guanosine 5′-monophosphate positioned on a suitable site to coordinate with the lanthanide ion. The substitution of the coordination naphthyridine by the phosphate oxygen atoms caused obvious relaxivity decrease. The negligible cytotoxicity and appropriate blood circulation time of Gd**-ANAMD** allow potential application of Magnetic Resonance Imaging *in vivo*. $^1$H NMR confirmed that the selectivity of these lanthanide complexes towards guanosine was attributed to the formation of hydrogen bonds between the guanine moeity and the naphthyridine. The fluorescence detection and lifetime measurement of Tb**-ANAMD** and Eu**-ANAMD** suggested that the decrease of the relaxivity is not attributed to the change of the *q* value, but caused by the prolonging of the residence lifetime of inner-sphere water.



## 1. Introduction

Magnetic resonance imaging (MRI) offers the unique opportunity for biosensing due to its non-invasion and capability of producing three-dimensional representations of opaque organisms with high spatial and temporal resolutions [1–7]. The exciting frontier for MRI investigation is the development of responsive contrast agents that can be used to report chemical species and reactions of interest in living biological systems [8–10]. Since the fact that the "read-out" mechanism of MRI agents comes into play through the proton relaxation of water molecules, the noncovalent interactions acting as vital parts in the recognition processes would be seriously interfered with in aqueous medium [11–13]. The design of highly selective and effective "smart" MRI contrast agents for bio-molecules, i.e. nucleotides and nucleic acids, represents a judicious protocol.

On the other hand, a great deal of interest has been focused on the molecular recognition of nucleotide polyphosphates because they play a major role in understanding and evaluating several key biological processes [14–23]. While considerable efforts have been devoted to developing chemosensors for various nucleotides in the past decade [24], the improved sensor with the ability to distinguish guanosine 5′-monophosphate (GMP) from others is still urgently desired, since GMP is the signal transduction modulation molecule and the important intercellular signaling molecule [25,26]. Guanosine 5′-monophosphate is a fundamental part in the synthesis of nucleic acids and metabolic processes, as well as a neuroprotective agent against glutamate or oxygen/glucose deprivation induced neurotoxicity[27,28]. Inspired by the elegant smart contrast agents for the β-galactosidase activity described by Meade et al. [29,30], and adenosine based on aptamer-conjugated gadolinium complex [31], herein, we reported a new naphthyridine-based Gd(III) complex as magnetic resonance imaging contrast towards GMP through the incorporation of a 2-amino-7-methyl-1,8-naphthyridine to a Gd(III) platform. We envisioned that the incorporation of naphthyridine moiety would interact with guanine moiety through Watson–Crick base-pairing [32–34]; these interactions relieve steric congestion around the $Gd^{3+}$ center, allowing the phosphate with suitable positions to be coordinated, from which the improvement of the selectivity toward GMP over other ribonucleotide polyphosphates is expected. Furthermore, naphthyridine could also act as a sensitizer to lanthanide ion (Eu, Tb), pairing with guanine base, resulting in the luminescence change for the inhibited sensitizing process. Such could be the alternative sensing channel beside the

* Corresponding author. Tel./fax: +86 411 84986216.
*E-mail address:* cyduan@dlut.edu.cn (C. Duan).

0039-9140/$ - see front matter © 2013 Elsevier B.V. All rights reserved.
http://dx.doi.org/10.1016/j.talanta.2013.09.020

MRI, superior to the most other Gd-based small molecular contrast agents [29–31].

## 2. Experimental

### 2.1. Instruments and reagents

All reagents and solvents were of analytical reagent grade and were used without further purification unless otherwise stated.

### 2.2. Physical measurements

1H NMR spectra were measured on a VARIAN INOVA-400 spectrometer(Varian Corp., American) with chemical shifts reported as ppm (in $d_6$-DMSO, $CDCl_3$ or $D_2O$, TMS as internal standard). Electrospray ionization mass spectra (ESI-MS) were carried out on a high performance liquid chromatography (HPLC)-quadrapole(Q)-time of flight(Tof) MS spectrometer(Agilent Corp., America). The solution fluorescent spectra were measured on EDINBURGH FS920 (Edinburgh Corp., England). Optical absorption spectra were measured on a TU-1900 Uv/vis spectrophotometer (Beijing Purkinje General Instrument Corp., China) at room temperature. Reversed-phase chromatography was performed by Dalian Zhonghuida Scientific Instrument Company using C18 columns. Inductively Coupled Plasma Optical Emission Spectrometry(ICP-OES) was performed on a Perkin-Elmer Optima 2000 DV ICP-OES (Perkin-Elmer Corp., America). NMR imaging was performed on an NMR NMI-20 Analyst Analyzing & Imaging system (Shanghai Niumag Corp., China) using a 0.5 T magnet, point resolution = 256 × 128 mm, section thickness = 1 mm, TE = 23 ms, TR = 500 ms, and number of acquisitions = 4.

### 2.3. Luminescence spectral measurements

Stock solutions (10 mM) of the sodium salts of nucleotides of ADP(Adenosine-5′-diphosphate disodium), ATP (Adenosine-5′-triphosphate disodium trihydrate), AMP (Adenosine-5′-mono-phosphate acid monodydrate), CDP(Cytidine-5′-diphosphate disodium hydrate), CTP (Cytidine-5′-triphosphate disodium dihydrate), CMP (Cytidine-5′-diphosphate acid), GDP(Guanosine-5′-diphosphate disodium), GTP (Guanosine-5′-triphosphate disodium hydrate), GMP (Guanosine-5′-monophosphate disodium), UDP (Uridine-5′-diphosphate disodium), UTP (Uridine-5′-triphosphate trisodium), UMP (Uridine-5′-monophosphate disodium) in $H_2O$ solvents were prepared. Test solutions were prepared by placing 2 μL (10 μM) of host stock solution into a quartz cell of 1 cm optical path length including 2 mL distilled aqueous solution, and then adding an appropriate aliquot of each nucleotide stock by using a micro-syringe.

Luminescence measurements of the europium (III) and terbium (III) analogs were performed in the absence or presence of 1 equivalent GMP. Samples were excited at 345 nm, and the emission maximum at 544 nm was used to determine luminescence lifetimes. The number of bound water molecules was estimated as the reference [35].

### 2.4. Relaxivity measurements and MR imaging in vivo

All MR relaxivity measurements were performed on an NMR NMI-20 Analyst Analyzing & Imaging system (Shanghai Niumag Corp.). $T_1$-weighted MR images were acquired using a multi-slice gradient echo sequence. The specific relaxivity values of $r_1$ was calculated through the curve fitting of $1/T_1$ ($s^{-1}$) vs. the Gd concentration (mM). *In vivo* MR imaging experiments were performed using a 0.5 T systems. A 0.2 mL of the Gd-**ANAMD** (1 mM) and 0.5 mL of the Gd-**ANAMD** (10 mM) aqueous solution were injected into white mouse through subcutaneous injection and intraperitoneal injection, respectively.

### 2.5. Cytotoxicity assay

*In vitro* cytotoxicity was measured by performing methyl thiazolyl tetrazolium (MTT) assays on the MCF-7 cells (a human breast cancer cell line). Cells were seeded into a 96-well cell culture plate at $5 \times 10^4$/well, under 100% humidity, and were cultured at 37 °C and 5% $CO_2$ for 24 h. Then, the cells were incubated with Gd-**ANAMD** (0, 20, 50,150, 250 and 400 μM) in Dulbecco's modified eagle medium for 24 h at 37 °C under 5% $CO_2$. Thereafter, MTT (5 mg/mL) was added to each well and the plate was incubated for an additional 4 h at 37 °C under 5% $CO_2$. After the addition of DMSO, the assay plate was allowed to stand at room temperature for 2 h. The OD 570 value (Abs.) of each well, with background subtraction at 690 nm, was measured by means of a Tecan Infinite M200 monochromator-based multifunction microplate reader. The Eq. (A.2) was used to calculate the inhibition of cell growth.

### 2.6. Crystallography

Intensity data of compound Tb-**ANAMD** was collected on a BRUKER SMART APEXCCD diffractometer with graphite-monochromated Mo-Kα ($\lambda = 0.71073$ Å) using the SMART and SAINT programs. Crystal data for Tb-**ANAMD** are: $[Tb(C_{25}H_{32}N_7O_7)] \cdot 5.5H_2O$, Monoclinic C2/C, $a = 40.543(2)$ Å, $b = 11.0269(7)$ Å, $c = 14.2239(8)$ Å, $V = 6210.2(6)$ Å$^3$, $T = 200(2)$ K, $R_1 = 0.0320$, and $wR_2 = 0.0826$ for 5454 reflections with $I > 2\sigma(I)$. CCDC number 910635. All the non-hydrogen atoms were refined anisotropically. Except the solvent molecules, the hydrogen atoms within the ligand were fixed geometrically at calculated distances and allowed to ride on their parent non-hydrogen atoms with the isotropic displacement being fixed at 1.2 and 1.5 times of the attached atoms .

### 2.7. Preparation of compounds

Ligand **$H_3$ANAMD** was synthesized according to the synthetic route outlined in Fig. 1. The nucleophilic substitution of 2-(N-methoxycarbonyl) amino-7-bromomethyl-1,8-naphthyridine was reacted with **1** to give **2** in a yield of 56%. **2** was then treated with trifluoroacetic acid to remove the protecting groups and followed by reacting with $Gd(NO_3)_3 \cdot 6H_2O$. The product Gd-**ANAMD** was purified *via* semi-preparatory high performance liquid chromatography (HPLC) on a reversed phase column. The purity and identity of the collected fractions were confirmed by the analytical HPLC-MS, and the $Gd^{3+}$ content was analyzed with inductively coupled plasma optical emission spectroscopy.

#### 2.7.1. Synthesis of N-(7-methyl-[1,8]naphthyridin-2-yl)-acetamide[36]

2-amino-7-methylnaphthyridine (2.5g, 15.7 mmol) was dissolved in 25 mL dry acetic anhydride and refluxed 8 h. Solvent was removed under vacuum. The crude product was purified by column chromatography using 50% ethyl acetate in petroleum ether to give pale yellow solid (2.2 g, 70% yield): $^1$H NMR (400 MHz, $CDCl_3$) $\delta$ 8.92 (s, 1H), 8.47 (d, 1H $J = 8.8$ Hz ),8.16 (d, 1H $J = 8.8$ Hz ), 8.05 (d, 1H $J = 8.8$ Hz ), 7.31 (d, 1H), 2.8 (s, 3H ) 2.30 (s,3H).

#### 2.7.2. Synthesis of 2-(N-methoxycarbonyl)amino-7-bromomethyl-1,8-naphthyridine[37,38]

Solution of N-(7-Methyl-[1,8]naphthyridin-2-yl)-acetamide (0.88 g, 4.00 mmol), NBS (0.84 g, 4.80 mmol), and benzoyl peroxide in a

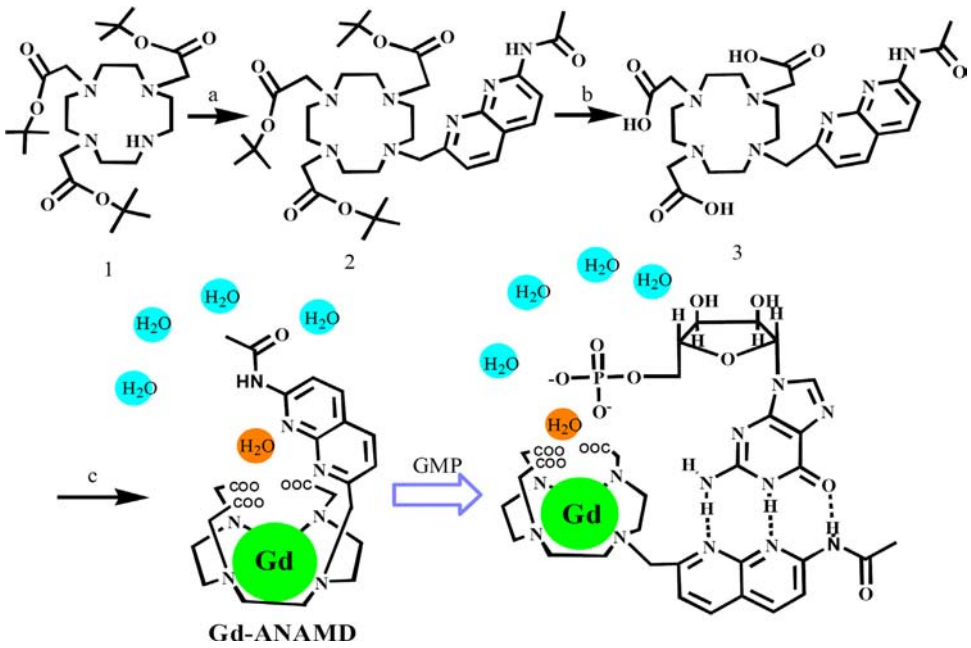


**Fig. 1.** Synthetic procedure of Gd-**ANAMD** and its responsing mechanism for GMP. (a) 2-(N-methoxycarbonyl) amino-7-bromomethyl-1,8-naphthyridine/DMF, reflux (56%); (b) trifluoroacetic acid, $CH_2Cl_2$, (79%); and (c) Gd-$(NO_3)_3 \cdot 6H_2O$, MeOH/$H_2O$, (50%).

mixture of chloroform and acetonitrile (5:4) was heated to reflux. Reactions were monitored by TLC. After the reaction mixture had been cooled, the solvent was evaporated. The residue was dissolved in chloroform, washed with water three times, dried over $Na_2SO_4$, and evaporated to get a yellow-brown solid. Purification on silica gel column chromatography using ethyl acetate/petroleum ether (from1:2 to 2:1 *v/v*) gave products (light-yellow solid, 0.176 g, 16%). $^1$H NMR ($CDCl_3$, 400 MHz): $d$=8.58 (d, 1H, $J$=9.0 Hz), 8.27 (d, 1H, $J$=8.8 Hz), 8.19 (d, 1H, $J$=8.3 Hz), 7.65 (d, 1H, $J$=8.3 Hz), 4.70 (s, 2H), 2.35 ppm (s, 3H).

### 2.7.3. 1,4,7-tri(tert-butoxymethane)-1,4,7,10-tetraazacyclododecane (t-Bu-DO3A) (1)[39,40]

1,4,7,10-tetraazacyclododecane (cyclen) (2.5 g, 14.53 mmol) and $NaHCO_3$(4.028 g, 47.95 mmol) were added to dry acetonitrile (60 mL) and stirred at 0 °C under an atmosphere of nitrogen. t-Butyl bromoacetate (8.5027 g, 47.95 mmol) was added slowly from a dropping funnel in 2 h at 0 °C. After complete addition, the mixture was allowed to stir over 48 h. The resulting precipitate was filtered off and washed with MeCN. The filtrate was evaporated under reduced pressure to leave a solid white product. The product was recrystallized using hot toluene to give a white solid (4.1 g, 55%). $^1$H NMR (400 MHz, $CDCl_3$) $\delta$ 1.49 (27H, s, tert-butyl $CH_3$), 2.59 (4H, bs, $NCH_2$), 2.93 (8H, bs, $NCH_2$), 3.10 (4H, bs, $CH_2$), 3.29 (2H, s, $COCH_2N$), 3.38 (4H, s, $COCH_2N$), 10.12 (1H, NH). API-EI (+)515.5.

### 2.7.4. [7-(7-acetylamino-[1,8]naphthyridin-2-ylmethyl)-1,4,7-tri-tert-butoxycarbonylmethyl-1,4,7,10 tetraaza-cyclododec-1-yl]-acetic acid tert-butyl ester (2)

To compound N-(7-bromomethyl-[1,8]naphthyridin-2-yl)-acetamide (1.0 g, 1.94 mmol, 1.0 equiv.) and t-Bu-DO3A (0.64 g, 2.30 mmol, 1.1 equiv.) in $CH_3CN$/DMF (2:1 *v/v* ) was added $Cs_2CO_3$ 0.9508g (1.5 equiv. ), and the reaction mixture was heated to 60 °C for 24 h under argon. After cooling to room temperature, the resulting precipitate was filtered off and washed with MeCN. The filtrate was diluted with EtOAc, washed with $H_2O$ and brine, dried over $MgSO_4$, and concentrated to give yellow oil. The product was recrystallized using EtOAc to give a white solid (0.7845 g, 56.5%). $^1$H NMR (400 MHz, $CDCl_3$) $\delta$ 10.20 (s, 1H); 8.49 (d, 2H); 8.09 (t, 2H), 7.37 (d, 2H), 3.90 (s, 2H), 3.20 (d, 4H),2.92(s,2H),2.63 (bs, 9H), 2.42 (s, 6H), 1.78 (bs, 5H), 1.47 (s, 9H), 1.27 (s, 18H). TOF-ESI-MS. Calcd. for $[M+H]^+$ 714.4554. Found: *m/z*: 714.2565. Calcd. for $[M+2H]^{2+}$ 357.7316. Found: *m /z*: 357.6277.

### 2.7.5. [7-(7-acetylamino-[1,8]naphthyridin-2-ylmethyl)-1,4,7-tri–carboxymethyl-1,4,7,10tetraaza-cyclododec-1-yl]-acetic acid (H3ANAMD) (3)

A solution of trifluoroacetic acid (1.5 mL) in $CH_2Cl_2$ (2 mL) was added dropwise to a solution of compound 2 (200 mg, 0.19 mmol) in $CH_2Cl_2$. The resulting solution was stirred for 24 h, and the solvent was removed by rotary evaporation. The residue was dissolved in 1 mL of MeOH, followed by dropwise addition of diethyl ether at 0–5 °C, the solid was filtered and washed with cold ethyl ether (3 × 10 mL), giving compound 4 as a pale yellow solid (80 mg, 52.6%). $^1$H NMR (400 MHz, $CD_3OD$ ) $\delta$ 8.34(d,1H), 8.24(d, 1H), 7.92(d, 1H), 7.42(d, 1H), 4.01(d, 2H), 3.87(bs, 4H), 3.67(m, 4H), 3.52(m, 2H), 3.32 – 3.01(m, 16H), 2.28(s, 3H), TOF-ESI-MS. Calcd. for $[M+H]^+$: *m/z* 546.2676. Found: *m/z* 546.3442. $[M+Na]^+$: *m/z* 568.2496. Found: *m/z* 568.3301.

### 2.7.6. Synthesis of Gd-ANAMD

Gd-**ANAMD** were prepared by dissolving **$H_3$ANAMD** (50 mg, 0.092 mmol) and 1.10 equiv. of the Gd$(NO_3)_3 \cdot 6H_2O$ in a solution of methanol and water (1:1, v/v). The pH was adjusted to 5.5 with 1 M NaOH, and the mixture was stirred for 24 h at room temperature. After the mixture was evaporated to dryness, the residue was dissolved in distilled water (2 mL) and further purified by reversed-phase chromatography. The Gd content was measured using ICP-OES. TOF-ESI-MS: calcd. for $[M+Na\ ]^+$: *m/z* 723.1470. Found: *m/z* 723.1194.

Ln-**ANAMD** (Tb, Eu) was prepared by similar procedures, TOF-ESI-MS: calcd. for [Tb-**ANAMD**+Na]$^+$: *m/z* 724.1514. Found: *m/z* 724.1760; Calcd. for [**Eu-ANAMD**+H]$^+$: *m/z* 696.1640. Found: *m/z* 696.1533 and [Eu-**ANAMD** +Na]$^+$: *m/z* 718.1459. Found: *m/z* 718.1461.

## 3. Results and discussion

### 3.1. Characterization of Gd-ANAMD

Electrospray MS(ESI-MS) of Gd-**ANAMD** in aqueous solution exhibits a simple peak at *m/z* 723.1194, assignable to [Na(Gd-**ANAMD**)]$^{+}$, according to the exact comparison of the peak with the simulation on the basis of natural isotopic abundances. Testing with xylena orange for complex solution of pH=6 indicates the absence of free $Gd^{3+}$, further confirming its stability in the aqueous solution. And so are the isomorphism compounds Ln-**ANAMD** (Ln=Tb, Eu). Single crystal X-ray structure analysis of Tb compounds revealed that each Tb(III) ion was coordinated by three carboxyl oxygen atoms on the three arms and four nitrogen atoms of the macrocycle, one nitrogen atom of naphthyridine and one water molecule to complete the nine-coordinate geometry, which is common in all commercial DOTA-like contrast agents[41,42]. The hydrogen bonding trigger in N-(7-Methyl-[1,8]naphthyridin-2-yl)-acetamide did not cap over the Gd-DOTA moiety( see Fig. 2), and could form strong multihydrogen bonds with guanosine *via* Watson–Crick base-pairing, such results in the change of the coordination environment of the lanthanide ion and leads to the obvious magnetic resonance responding variations.

### 3.2. Magnetic resonance responses towards GMP.

Gd-**ANAMD** exhibits relative stable relaxivity ($r_1$=5.48 $mM^{-1}$ $s^{-1}$) in HEPES buffer at pH 7.4, which is relatively higher than the commercial Gd-DOTA-like CAs (3.5−4.8 $mM^{-1}$ $s^{-1}$), suggesting that at least one inner-sphere water molecule was bonded to the lanthanide ion[42]. Upon the addition of GMP up to 1 mM into the HEPES buffer containing Gd-**ANAMD** (1 mM), the relaxivity decreased to 2.85 $mM^{-1}$ $s^{-1}$ (curve graph in Fig. 3). The titration plot upon the addition of GMP exhibited the apparent $K_A$ ca $4.6\times10^4$ $M^{-1}$ for the 1:1 GMP/Gd-**ANAMD** complexation species. The observed relaxivity decrease for Gd-**ANAMD** was stable over time, indicating that Gd-**ANAMD** has excellent stability and remains intact in the presence of GMP. The acquired $T_1$ weighted images of Gd-**ANAMD** (1 mM) with a commercial 0.5 T magnet in the absence and presence of GMP readily visualized differences in a biologically relevant micromolar range.

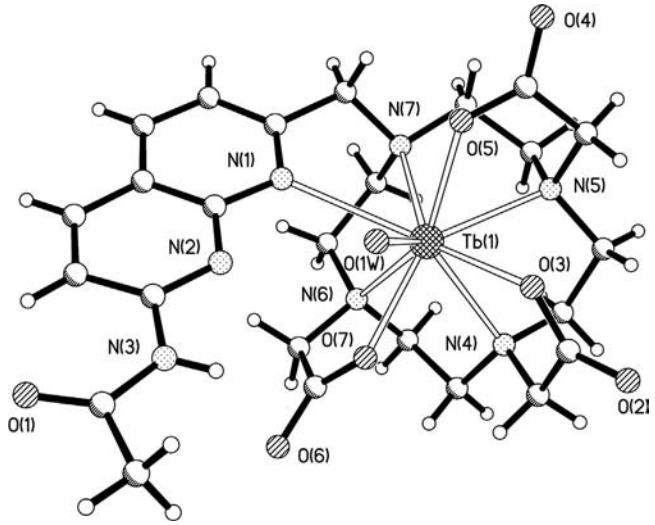


**Fig. 2.** Molecular structure of Tb-**ANAMD** showing the coordination geometry of the lanthanide ion. Solvents are omitted for clarity. Important bond distances (Å): Tb(1)–O(5) 2.308(3), Tb(1)–O(7) 2.324(3), Tb(1)–O(3) 2.333(3), Tb(1)–O(1W) 2.436 (3), Tb(1)–N(4), 2.622(4), Tb(1)–N(5) 2.653(4), Tb(1)–N(7) 2.657(4), Tb(1)–N(6) 2.675(4), and Tb(1)–N(1), 2.675(4).

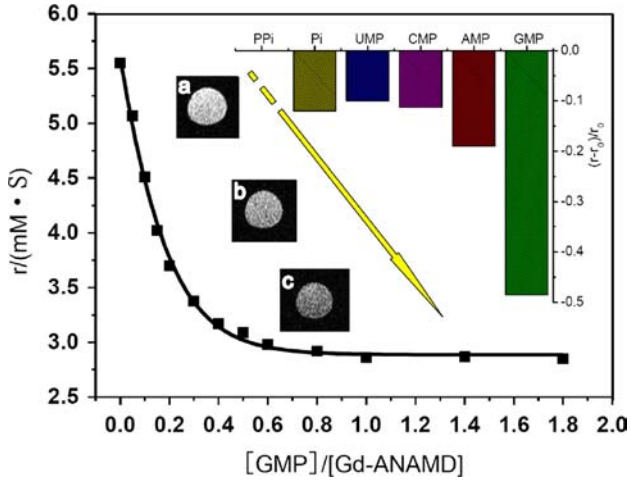


**Fig. 3.** Relaxivity change profile of Gd-**ANAMD** (1 mM) in HEPES buffer solution (pH=7.4, 50 mM) upon addition of GMP. (a) Gd-**ANAMD**; (b) Gd-**ANAMD**+0.4 mM GMP; and (c) Gd-**ANAMD**+0.8 mM GMP.

The relaxivity changes of Gd-**ANAMD** (1 mM) towards GMP are special in the aqueous media. The addition of other nucleotide monophosphates and guanosine polyphosphates hardly changed the relaxivity (column graph in Fig. 3). As reported in the references [43–45], the high selectivity should be attributed to the strongly multi-hydrogen bonds formation between the guanosine and aminonaphthyridine *via* the Watson–Crick base-pairing, resulting that the phosphate group in GMP sited on a suitable position to coordinate with the lanthanide ion.

In terms of responsive Gd-based MRI agent design, three main factors could be used to modulate relaxivity: the number of inner-sphere water molecules ($q$); the rotational tumbling time ($\tau_R$) and the residence lifetime of inner-sphere water molecules ($\tau_m$). Most prevalently, contrast agent sensors display a change in $q$ in response to a particular analyte [29,30]. The second always attributes to the contrast agent weight change because of the associative or dissociative process between the contrast agents and analytes [31,46]. Finally, tuning water exchange rate ($1/\tau_m$) of nine-coordinate responsive Gd-based constrast agents to invoke a significant relaxivity change involves several factors: steric crowding, coordination geometry and counter ion [47]. As far as we know few reports on responsive contrast agent are based on the tuning water exchange rate because how to delicately modulate the factors by using the analytes to attain the relaxivity change baffles the responsive contrast agent design. In this case, the phosphate group could lead to a slow rate of water exchange due to defining the water structure around the coordinated water molecule and the relieving steric congestion around the $Gd^{3+}$ center, according to the reference [47,48]. It is speculated that the decrease of the relaxivity upon the addition of GMP should be attributed to either the decreased number of the coordination water molecules ($q$) or the prolonging of the residence lifetime of inner-sphere water ($\tau_m$).

### 3.3. Mechanism

Eu-**ANAMD** exhibits characteristic $Eu^{3+}$ emissions assignable to the transitions of $^5D_0\rightarrow{}^7F_1$, $^5D_0\rightarrow{}^7F_2$ and $^5D_0\rightarrow{}^7F_4$ when excited at 350 nm [49]. Upon the addition of GMP solution, the luminescence intensities of Eu-**ANAMD** decrease gradually (Fig. S1). Time dependence luminescence measurements demonstrated that the life time of the emission at 610 nm is about 0.56 ms in aqueous solution. And with the substituted $D_2O$ solution, the life time of the same emission increased to 1.96 ms, and gave the number of

inner-sphere water molecules $q$ about 1.24 [35]. In the presence of GMP, the life time of the emission at 610 nm is about 0.55 ms in aqueous solution, and the replacement of $H_2O$ solution by $D_2O$ increases the life time to 1.55 ms, with the $q$ value calculated as 1.12. The small $q$ decrease suggested that the decrease in relaxivity was hardly attributed to the variation of the $q$ value, but attributed to the prolonged residence lifetime of inner-sphere water. In fact, the water exchange rate ($k_{ex}$, 298.15 K) at the Gd center was about $2.6\times10^6\ s^{-1}$ assessed by the well established VT $^{17}O$ NMR procedure [50], and the presence of GMP caused the water exchange rate ($k_{ex,\ 298.15\ K}=4.5\times10^4\ s^{-1}$) at the Gd center prolonged significantly. It should be concluded that the decrease of exchange rate of the coordinated water was the important factor for the decrease of the relaxivity of Gd-ANAMD upon the addition of GMP.

$^1H$ NMR spectra of Eu-**ANAMD** (5 mM) exhibited four broad naphthyridine Ar–H signals at about 12.0–13.0 ppm in DMSO/$D_2O$ (4/1,v/v) solution [47]. The addition of GMP caused the small but significant upfield shifts (ca. 0.1–0.3 ppm) of these protons. Two new peaks appeared at about 8.62 and 5.02 ppm were assigned to the two kinds of N–H protons on the guanine base. They did not appear in the NMR spectrum of GMP due to the fast proton exchange with $D_2O$. The appearance could be assignable to the formation of strong hydrogen bond with the naphthyridine (the left part of Fig. 4). At the mean time, the peak on the $^{31}P$ NMR of GMP at $\delta=3.16$ ppm also shifted to 2.25 ppm in the presence of Eu-**ANAMD**, suggesting the potential coordination of the phosphate oxygen atom to the Eu(III) ion [51] (the right part of Fig. 4). In this case, it should be concluded that the selectivity of these lanthanide complexes towards GMP was attributed to the formation of hydrogen bonds between the guanine base and the naphthyridine, and also the coordination of the phosphate oxygen atom to lanthanide ion.

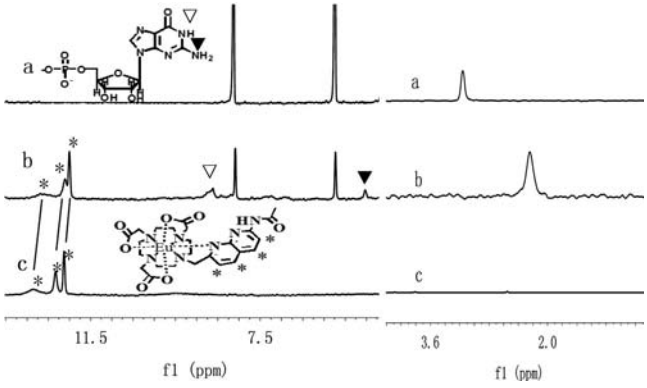


**Fig. 4.** Partial $^1H$ NMR (left picture) and $^{31}P$ NMR (right picture) spectra for (a) GMP (5 mM), (b) Eu–**ANAMD** (5 mM)+GMP (5 mM), and (c) Eu-**ANAMD** (5 mM) in d6-DMSO/$D_2O$ (4/1, v/v), respectively.

### 3.4. Fluorescence detection of Tb-ANAMD towards GMP

As indicated in Fig. 5 (the left part), Tb-**ANAMD** shows four Tb-characterized emission bands at 490, 546, 583, and 621 nm, corresponding to the transition from the $^5D_4$ excited state to the $^7F_6$, $^7F_5$, $^7F_4$, and $^7F_3$ ground state, respectively [49]. The addition of GMP significantly quenches the green color emission of Tb-**ANAMD** and the titration curve suggested the formation of 1:1 complexation species with the association constant (log $K_{ass}$) calculated as 3.2. The responses of Tb-**ANAMD** towards GMP were pH independent over the range of 5.0–9.0, (Fig. S2) and the presence of other nucleotides and phosphates did not affect the luminescent responses (the right part of Fig. 5). It should attribute to the good matching of naphthyridine and guanine, which favors photoelectron transfer (PET) from the guanine to the naphthyridine, thereby preventing energy transfer from the antenna (naphthyridine) to the lanthanide and consequently quenching terbium luminescence with excellent selectivity [52]. The good matching of naphthyridine and guanine also leads to the coordination of phosphate to substitute the naphthyridine upon the

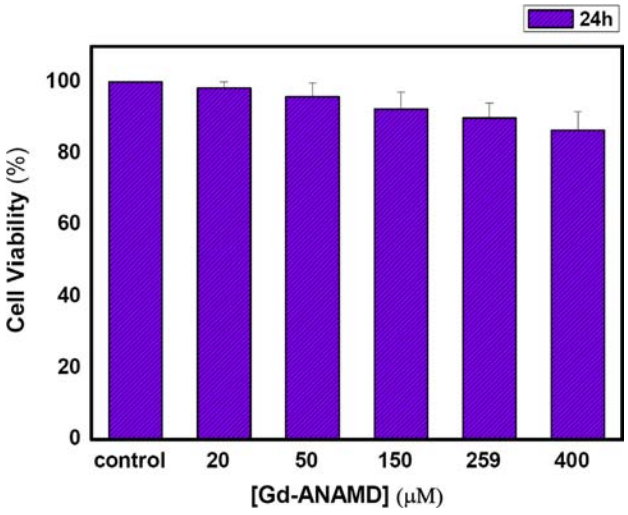


**Fig. 6.** Cell viability of MCF-7 cells incubated with Gd-**ANAMD** at different concentrations for 24 h *in vitro*.

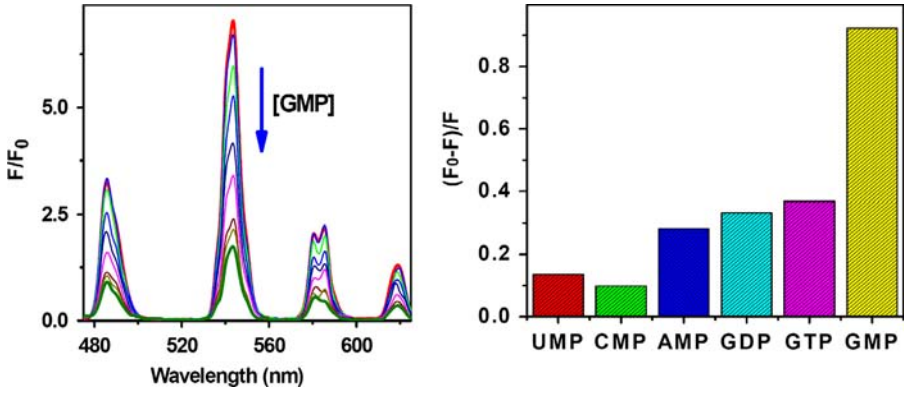


**Fig. 5.** Left: family of emission spectra of Tb-**ANAMD** (20 μM) upon addition of GMP up to 0.5 mM. Right: the luminescence responses of Tb-**ANAMD** (20 μM) towards nucleotides (0.5 mM) interested, excitation at 345 nm, the intensities were recorded at 546 nm.

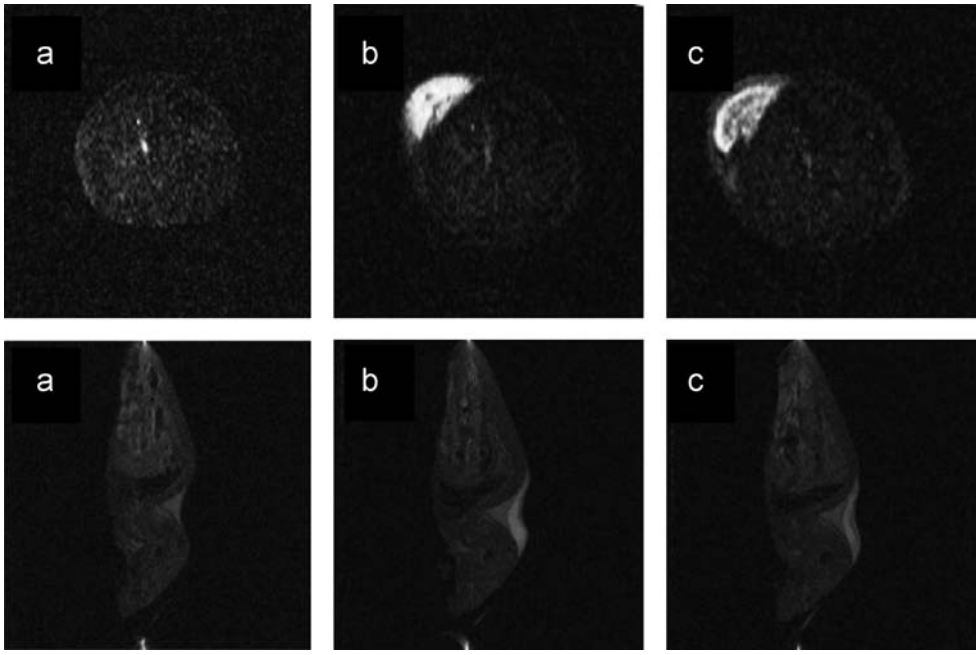


**Fig. 7.** $T_1$-weighted MR Transection images (top) and Sagittalsection images (bottom) of a living mouse None (a); Gd-**ANAMD**(0.2 mL, 0.25 mM) (b) and Gd-**ANAMD**+GMP (0.2 mL, 0.25 mM) (c).

addition of GMP and consequently causes a slow rate of water exchange.

The fluorescence decay rates of Tb (III) analog in water and $D_2O$ with and without GMP present were also measured to calculate the number of inner-sphere water molecules ($q$). The increase of life time from 1.85 to 3.23 ms with the $D_2O$ substituted the $H_2O$ solution gave the $q$, the number of inner-sphere water molecules about 0.92. Whereas, the increase of life time from 1.71 to 2.72 ms in the presence of 1 equivalent GMP with the $D_2O$ substituted the $H_2O$ solution gave the $q$ value of about 0.86. It coincides well with the $q$ value which is detected according to the lifetime measurements of europium, and reconfirms that the important factor for the decrease of the relaxivity of Gd-**ANAMD** should be the decrease of exchange rate of the coordinated water, and not the change of the number of inner-sphere water molecules ($q$).

### 3.5. *The study of Gd-ANAMD in vivo*

Since the MRI contrast agents were eventually used in living body, the cytotoxicity of Gd-**ANAMD** was evaluated *via* a MTT assay of viability of MCF-7. As shown in Fig. 6, upon incubation with various concentrations of Gd-**ANAMD** (Ga) for 24 h, fewer than 10% of the MCF-7 cells died. Even at the concentration of 0.4 mM of Gd-**ANAMD**, the cell viability still remained about 90%, which exceeds the dose used in the conventional clinical Gd-based MRI contrast agent in patients (0.05–0.3 mM $kg^{-1}$), indicating negligible cytotoxic of Gd-**ANAMD** at the given concentration range.

The subcutaneous injection of suitable dose Gd-ANAMD on white mouse modes following by the administration of equal GMP caused the $T_1$-weight MR images of the interest portions to exhibit significant bright effect on a commercial 0.5 T Animal MRI (Fig. 7). The successive bright MRI action of the Gd-ANAMD on white mouse model (10 g) was achieved at different time points, even after 24 h by intraperitoneal injection of a relatively big dose (0.5 mL, 10 mM), suggesting that the contrast agents could continuously improve contrast in tissues and have a relatively longer blood circulation time.

## 4. Conclusions

In conclusion, we have designed and demonstrated a new responsive $T_1$-weighted MR imagining contrast agent for GMP. The formation of strong multihydrogen bonds between naphthyridine and guanosine made the phosphate in GMP positioned on a suitable site to coordinate with the lanthanide ion. The substitution of the coordination naphthyridine by the phosphate oxygen atoms caused obvious relaxivity decrease. The fluorescence detection and lifetime measurement of Tb-**ANAMD** and Eu-**ANAMD** suggested that the decrease of the relaxivity is not attributed to the change of the $q$ value, but caused by the prolonging of the residence lifetime of inner-sphere water. The contrast agent exhibits negligible cytotoxicity and appropriate blood circulation time which ensures the potential to imagine *in vivo*. Since neurotrosis was accompanied with the GMP accumulation in the extracellular space, such a contrast agent could be served as potential diagnostic reagent for nerve injuries.

## Acknowledgments

The authors thank the National Basic Research Program of China (2013CB733702) and NSFC (21102014).

## Appendix A. Supplementary material

Supplementary data associated with this article can be found in the online version at http://dx.doi.org/10.1016/j.talanta.2013.09.020.

## Reference

[1] P. Caravan, Chem. Soc. Rev. 35 (2006) 512–523.
[2] T.J. Meade, S. Aime, Acc. Chem. Res. 42 (2009) (821–821).
[3] L.M. De Leon-Rodriguez, A.G.M. Lubag, C.R. Malloy, G.V. Martinez, R.J. Gillies, A. D. Sherry, Acc. Chem. Res. 42 (2009) 948–957.
[4] M. Woods, D.E. Woessner, A.D. Sherry, Chem. Soc. Rev. 35 (2006) 500–511.
[5] J. Cheon, J.H. Lee, Acc. Chem. Res. 41 (2008) 1630–1640.
[6] J.L. Major, T.J. Meade, Acc. Chem. Res. 42 (2009) 893–903.
[7] F. Adams, C. Barbante, Talanta 102 (2012) 16–25.

[8] E.L. Quea, C.J. Chang, Chem. Soc. Rev. 39 (2010) 51–60.
[9] A.C. Esqueda, J.A. López, G. Andreu-de-Riquer, J.C. Alvarado-Monzón, J. Ratnakar, A.J.M. Lubag, A.D. Sherry, L.M. De León-Rodríguez, J. Am. Chem. Soc. 131 (2009) 11387–11391.
[10] J. Luo, W.S. Li, P. Xu, L.Y. Zhang, Z.N. Chen, Inorg. Chem. 51 (2012) 9508–9516.
[11] M.W. Wong, M.J. Frisch, K.B. Wiberg, J. Am. Chem. Soc. 113 (1991) 4173–4184.
[12] J. Tomasi, M. Persico, Chem. Rev. 94 (1994) 2027–2094.
[13] K. Yoshimoto, S. Nishizawa, M. Minagawa, N. Teramae, J. Am. Chem. Soc. 125 (2003) 8982–8983.
[14] A. Ojida, I. Takashima, T. Kohira, H. Nonaka, I. Hamachi, J. Am. Chem. Soc. 130 (2008) 12095–12101.
[15] D.H. Lee, S.Y. Kim, J.I. Hong, Angew. Chem. Int. Ed. 43 (2004) 4777–4780.
[16] H.M. Wu, C. He, Z.H. Lin, Y. Liu, C.Y. Duan, Inorg. Chem. 48 (2009) 408–410.
[17] P.P. Neelakandan, M. Hariharan, D. Ramaiah, J. Am. Chem. Soc. 128 (2006) 11334–11335.
[18] S.L. Wang, Y.T. Chang, J. Am. Chem. Soc. 128 (2006) 10380–10381.
[19] J.Y. Kwon, N.J. Singh, H.N. Kim, S.K. Kim, K.S. Kim, J. Yoon, J. Am. Chem. Soc. 126 (2004) 8892–8894.
[20] X.Q. Chen, M.J. Jou, J. Yoon, Org. Lett. 11 (2009) 2181–2184.
[21] A. Kobori, S. Horie, H. Suda, I. Saito, K. Nakatani, J. Am. Chem. Soc. 126 (2004) 557–562.
[22] K. Nakatani, S. Sando, I. Saito, Bioorg. Med. Chem. 9 (2001) 2381–2385.
[23] K. Nakatani, S. Sando, H. Kumasawa, J. Kikuchi, I. Saito, J. Am. Chem. Soc. 123 (2001) 12650–12657.
[24] Y. Zhou, Z. Xu, J. Yoon, Chem. Soc. Rev. 40 (2011) 2222–2235.
[25] R.D. Fields, G. Burnstock, Nat. Rev. Neurosci. 7 (2006) 423–436.
[26] H. Decker, S.S. Francisco, C.B. Mendes-de-Aguiar, L.F. Romao, C.R. Boeck, A. G. Trentin, M.V. Neto, C.I. Tasca, J. Neurosci. Res. 85 (2007) 1943–1951.
[27] I.J.L. Oliveira, S. Molz, O.D. Souza, C.I. Tasca, Cell. Mol. Neurobiol. 22 (2002) 335–344.
[28] S.P. Oleskovicz, M.C. Martins, R.B. Leal, C.I. Tasca, Neurochem. Int. 52 (2008) 411–418.
[29] R.A. Moats, S.E. Fraser, T.J. Meade, Angew. Chem. Int. Ed. 36 (1997) 726–728.
[30] A.Y. Louie, M.M. Huber, E.T. Ahrens, U. Rothbacher, R. Moats, R.E. Jacobs, S. E. Fraser, T.J. Meade, Nat. Biotechnol. 18 (2000) 321–325.
[31] W. Xu, Y. Lu, Chem. Commun. 47 (2011) 4998–5000.
[32] K. Nakatani, S. Sando, I. Saito, J. Am. Chem. Soc. 122 (2000) 2172–2177.
[33] C. Dohno, S. Uno, K. Nakatani, J. Am. Chem. Soc. 129 (2007) 11898–11902.
[34] S. Nishizawa, K. Yoshimoto, T. Seino, C. Xu, M. Minagawa, H. Satake, A. Tong, N. Teramae, Talanta 63 (2004) 175–179.
[35] A. Beeby, I.M. Clarkson, R.S. Dickins, S. Faulkner, D. Parker, L. Royle, A.S. de Sousa, J.A.G. Williams, M. Woods, J. Chem. Soc., Perkin Trans. 2 (1999) 493–504.
[36] S. Goswami, R. Mukherjee, R. Mukherjee, S. Jana, A.C. Maity, A.K. Adak, Molecules 10 (2005) 929–936.
[37] H. He, M. Hagihara, K. Nakatani, Chem. Eur. J. 15 (2009) 10641–10648.
[38] T.R. Kelly, G.J. Bridger, C. Zhao, J. Am. Chem. Soc. 112 (1990) 8024–8034.
[39] J. Tanwar, A. Datta, A.K. Tiwari, S. Chaturvedi, H. Ojha, M. Allard, N. K. Chaudary, M. Thirumal, A.K. Mishra, Dalton Trans. 40 (2011) 3346–3351.
[40] A. Dadabhoy, S. Faulkner, P.G. Sammes, J. Chem. Soc., Perkin Trans. 2 (2002) 348–357.
[41] S.M. Cohen, J. Xu, E. Radkov, K.N. Raymond, Inorg. Chem. 39 (2000) 5747–5756.
[42] P. Caravan, J.J. Ellison, T.J. McMurry, R.B. Lauffer, Chem. Rev. 99 (1999) 2293–2314.
[43] R. Nishiyabu, N. Hashimoto, T. Cho, K. Watanabe, T. Yasunaga, A. Endo, K. Kaneko, T. Niidome, M. Murata, C. Adachi, M.Y.K. Hashizume, N. Kimizuka, J. Am. Chem. Soc. 131 (2009) 2151–2158.
[44] J. Liu, M. Morikawa, N. Kimizuka, J. Am. Chem. Soc. 133 (2011) 17370–17374.
[45] B. McMahon, P. Mauer, C.P. McCoy, T.C. Lee, T. Gunnlaugsson, J. Am. Chem. Soc. 131 (2009) 17542–17543.
[46] Zh. Zhang, M.T. Greenfield, M. Spiller, T.J. McMurry, R.B. Lauffer, P. Caravan, Angew. Chem. Int. Ed. 44 (2005) 6766–6769.
[47] S. Viswanathan, Z. Kovacs, K.N. Green, S.J. Ratnakar, A.D. Sherry, Chem. Rev. 110 (2010) 2960–3018.
[48] A.L. Thompson, D. Parker, D.A. Fulton, J.A.K. Howard, S.U. Pandya, H. Puschmann, K. Senanayake, P.A. Stenson, A. Badari, M. Botta, S. Avedanob, S. Aime, Dalton Trans. 47 (2006) 5605–5616.
[49] J.G. Bunzli, Chem. Rev. 110 (2010) 2729–2755.
[50] D.H. Powell, O.M. Ni Dhubhghaill, D. Pubanz, L. Helm, Y.S. Lebedev, W. Schlaepfer, A.E. Merbach, J. Am. Chem. Soc. 118 (1996) 9333–9346.
[51] AD. Sherry, J. Ren, J. Huskens, E. Bru1cher, E. Toth, C.F.C.G. Geraldes, M.M.C. A. Castro, W.P. Cacheris, Inorg. Chem. 35 (1996) 4604–4612.
[52] E.A. Weitz, J.Y. Chang, A.H. Rosenfield, V.C. Pierre, J. Am. Chem. Soc. 134 (2012) 16099–16102.